Journal of Materials Chemistry A

Accepted Manuscript

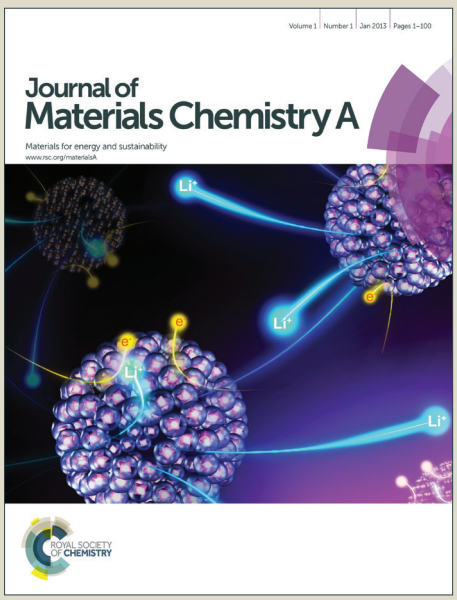

ROYAL SOCIETY OF CHEMISTRY

www.rsc.org/materialsA

Journal of Materials Chemistry A

Dynamic Article Links ►

Cite this: DOI: 10.1039/c0xx00000x

FULL PAPER

www.rsc.org/xxxxxx

Non-Solvent Processing for Robust but Thin Membrane of Ultra-High Molecular Weight Polyethylene †

Hiroki Uehara,*[a] Takuya Tamura,[a] Kazuki Hashidume,[a] Hidekazu Tanaka,[a] and Takeshi Yamanobe[a]

Received (in XXX, XXX) Xth XXXXXXXXX 20XX, Accepted Xth XXXXXXXXX 20XX

DOI: 10.1039/b000000x

Robust and thin membranes of ultra-high molecular weight polyethylene (UHWM-PE) were obtained from commercial powder material *via* melt-drawing technique without any solvent treatment. A combination of rolling and compressing successfully erases the powder boundaries within the initial films, which gives enables defect-free structure in a biaxially melt-drawn membrane. The resultant tensile strength was improved up to 90MPa, but the membrane thickness could be reduced into 6μm. Such membrane robustness and thinning are achieved by extended chain crystallization induced during biaxial melt-drawing.

Introduction

Ultra-high molecular weight polyethylene (UHMW-PE) has superior wear resistance[1,2] and biocompatibility,[3] thus is used for artificial knee joints and hip caps[4,5] with surface modifications for implantation.[6,7] Although these excellent properties originated from extremely long chains of UHMW-PE, its high melt viscosity due to many entanglements prevents manufacturing thin films or membranes. Therefore, some organic solvents which can dissolve PE, for example decahydronaphthalenedecalin and xylene, are used as plasticizer. This method is used for production of lithium ion battery separator.[8] Similar solvent dissolution is also beneficial for high-strength UHMW-PE fibre processing.[9-12] However, several tens of volume of these organic solvents toward UHMW-PE are required for disentangling UHMW-PE chains. These solvent vapours are hazardous to the environment and to the health of manufacturing personnel therefore must be collected necessarily, increasing processing costs.

Therefore, industries highly requires non-solvent processing of high-performance UHMW-PE membrane. One of the possible approach is reactor powder processing, which utilizes the less-entangled state of as-synthesized reactor powder. PE molecule exhibits the highest crystallization rate, due to the simplest architecture, thus immature shorter segments crystallize before complete chain growth on polymerization. This prevents molecules entangling even for the longer UHMW-PE chains, especially for slower chain growth at the lower polymerization temperature. Smith et al.[13] firstly applied such less-entangled reactor powder for film compaction below its melting temperature. The obtained film can be also solid-state tensile-drawn up to draw ratio (*DR*) of 20, exhibiting the maximum achievable tensile strength of 0.5GPa. Kanamoto et al.[14] combined the solid-state extrusion technique with subsequent solid-state tensile-drawing, giving the resultant tensile strength increases up to 1.5GPa. Rastogi et al.[15] further improved tensile strength up to 2.0GPa for selected UHMW-PE reactor powders. However, the ultra-drawing from the entangled powder is not successful, which restricts the wider availability of this drawing technique using reactor powder state.

In contrast, we have developed melt-drawing technique for manufacturing high-performance UHMW-PE films, utilizing the high viscosity of UHMW-PE melt attributed to its highly entangled state.[16-24] The advantage of this membrane manufacturing is its availability of various commercial UHMW-PE reactor powders. This methodology has also been applied for preparing transparent and robust films of poly(tetrafluoroethylene) (PTFE)[25] or poly poly(tetramethyl-*p*-silphenylenesiloxane) (PTMPS),[26] which exhibit similar high melt viscosity. During uniaxial melt-drawing of UHMW-PE, PTFE or PTMPS, the molecular disentanglement induces the oriented crystallization into extended-chain crystals (ECCs), resulting in high strength. Such melt-drawing is also applied to prepare biaxial membranes, yielding larger UHMW-PE and PTFE membranes with high performances.[27,28]

However, the adhesion between initial powders is often unsatisfied for latter drawing, thus this study adopts calendar-rolling to improve adhesion between reactor powders within the starting undrawn film.[29] Such a procedure also introduces molecular orientation that is desirable for uniaxial drawing along the rolling direction, but results in easy tearing along the perpendicular direction. This is disadvantageous for subsequent biaxial drawing for thinning the membrane. In the present study, such pre-orientation is eliminated by cross-stacking the rolled films, followed by compression moulding in the molten state. This procedure also prevents void formation caused by tearing the powder boundaries during biaxial drawing. The resultant properties of biaxially melt-drawn thin membranes were

characterized by mechanical tests. The membrane structure was also analysed by scanning electron microscopy (SEM), X-ray, and differential scanning calorimeter (DSC) measurements.

Experimental section

Film preparation

The UHMW-PE used was Hizex 340M supplied by Mitsui Chemical. Its viscosity average MW is 3.5×10^6 Da. This UHMW-PE material exhibits powder morphology with a diameter of about 150μm. The crystallinity estimated from fusion heat is 77%.[30] Initial film was continuously processed using a roll-processing machine with a parallel arrangement of two polished stainless-steel rolls 100mm in diameter and 150mm in width.[29] The distance between the two rolls was adjusted to 50μm, and 50 grams of reactor powder was placed between the two parallel rolls. Continuous rolling at 10rpm, corresponding to 3m/min for the resultant film length, produced the moulded films. The temperature of these two rolls was isothermally maintained at 145^{o}C, which is the optimum temperature for subsequent uniaxial drawing.[29] Squares with a 65mm x 65mm area were cut from the rolled films, and several films were assembled with alternate rolling directions, leading to cross-stacks. The number of assembled films depended on the desired thickness. This assembly of rolled film was sandwiched between commercial polyimide films (UPILEX-125S, Ube) and compression moulded into a film at 180^{o}C and 5MPa for 10min in a vacuum, followed by slow cooling to room temperature. A press equipped with a vacuum chamber (Boldwin, Japan) was used.[31] This film preparation innovated in this study is called as "roll-pressed" method here.

For comparison, other films were prepared directly from reactor powder without rolling, as in our previous study.[28] The reactor powder was sandwiched between commercial polyimide films and compression moulded into the film at 180^{o}C and 5MPa for 10min in a vacuum, followed by slow cooling to room temperature. This film preparation is called as conventional "powder-pressed" method in this study.

Biaxial Drawing

The above prepared UHMW-PE films were biaxially drawn at 150^{o}C up to a *DR* of 2x2 to 8x8. Such biaxial drawing along vertical and horizontal directions was performed simultaneously at a cross-head speed of 5mm/min. A custom-made machine was designed for such biaxial drawing.[28] The sample membrane was gripped by eight chucks with air-compression control to prevent slippage due to membrane thinning during drawing. Depending on the targeted *DR*, the initial sample films were cut to 20x20 to 40x40mm^2.

Measurements

The mechanical properties of the prepared membranes were measured by a Tensilon RTC-1325A tensile tester (A&D, Japan) at room temperature. Strips 5mm or 25mm wide and 50mm long were cut from the prepared membranes for tensile or tearing tests. Tensile tests were performed at a CHS of 20mm/min for 30mm gauge length. Tensile strength was calculated from the maximum recorded stress at the breaking point, and the tensile modulus was evaluated from the slope of the stress-strain curves.

Morphologies of the resultant membranes were observed using a Hitachi field-emission SEM S-4800 operated at 1.0kV. The sample membranes were uncoated for SEM morphological observations, so artifacts were negligible.

A Perkin-Elmer Diamond DSC was used for DSC measurement. Heating scans were performed from 50 to 180^{o}C at a rate of 10^{o}C/min in a nitrogen gas flow. The sample melting temperature (T_m) was evaluated as the peak temperature of the melting endotherm. Temperature and fusion heat were calibrated using indium and tin standards. A small amount of silicone oil was placed between the sample and the bottom of the DSC sample pan to avoid the effects of both shrinkage of the oriented membrane on melting and delay in heat transfer during heating scan.

Wide-angle X-ray diffraction (WAXD) measurements of the obtained membranes were performed using a Rigaku MicroMAX-007HF X-ray generator with a confocal multilayer mirror. The wavelength of the incident CuKα beam was 1.54 angstroms. The obtained WAXD patterns were recorded using a cooled CCD camera (Hamamatsu Photonics, C4742-98) with an image intensifier (Hamamatsu Photonics, V7739P). The incident beam was radiated perpendicular (through-view) or parallel (edge-view) to the membrane surface.

In-situ WAXD measurements were carried out during heating of the prepared membranes. The heating chamber[23,26] was installed in the beamline, and edge-viewed WAXD patterns were continuously recorded. The heating temperature range was 50 to 180^{o}C at a rate of 2^{o}C/min.

Results and Discussion

Biaxial drawing was performed at 150^{o}C because the maximum biaxial *DR* was obtained both for the "roll-pressed" films newly designed in this study, as well as for the conventional "powder-pressed" film prepared by simple compression molding of the reactor powder without roll processing. The appearances of these membranes were compared here. Fig. 1 presents photographs for *DR* = 8x8 membranes melt-drawn at 150^{o}C from the powder-pressed and roll-pressed films. The membrane thickness of both was 8μm. The biaxial melt-drawing of the powder-pressed film had a whitened membrane appearance, due to the morphological heterogeneity caused by the prior powder boundaries within the starting film. In contrast, a transparent membrane was obtained when the roll-pressed film was biaxially melt-drawn, indicating superior adhesion between the initial UHMW-PE powders. This result suggests that rolling is a key to obtaining homogeneity of the resultant biaxially melt-drawn membrane.

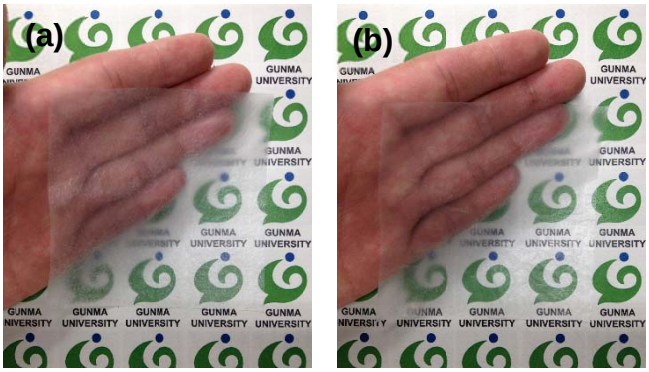

Fig 1 Comparison of photographs of *DR* = 8×8 membranes biaxially drawn at 150°C from the films prepared by (a) only compression-moulding of the initial UHMW-PE powder (powder-pressed series) and (b) combined calendar-rolling of the powder and subsequent compression-moulding (roll-pressed series).

Detailed morphologies of the resultant membranes were compared by SEM observation (Fig. 2). Both membranes biaxially melt-drawn from conventional power-pressed and newly-applied roll-pressed films exhibit the oriented fibrillar structure at the higher *DR*, corresponding to ECC formation. The amount of such ECCs increases with increasing biaxial *DR*, independent of initial film preparation. Also, lamellar crystals stack perpendicular to the former fibrils. Such a structural combination has been known as shish-kebab structure,[32] where folded-chain crystals (FCCs) epitaxially grow on the surface of ECC precursors. In the case of biaxial melt-drawing from the powder-pressed film, a development of fibrilar ECCs causes some flaws between them in Fig. 2C. These flaws are observable even for the undrawn film in Fig. 2A, indicating that they are originated from the powder boundaries. In contrast, biaxial melt-drawing from the roll-pressed film exhibits no surface tearing even for increasing

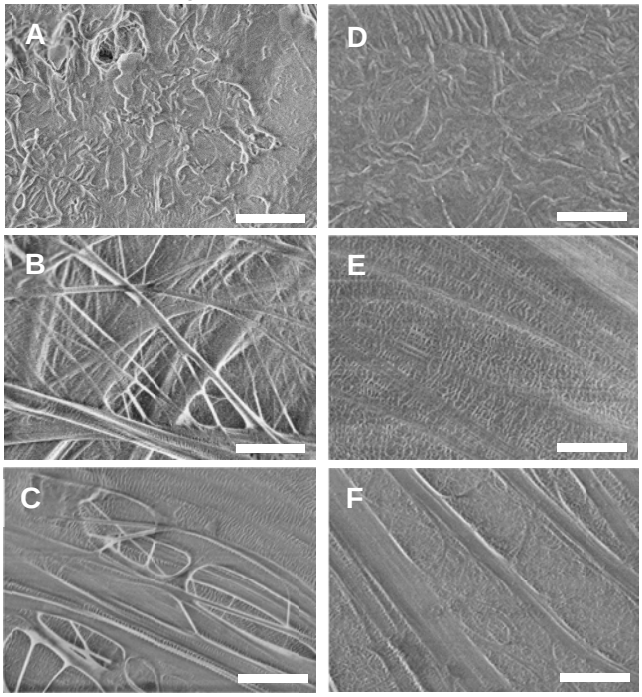

Fig 2 SEM images of the UHMW-PE membranes prepared from the powder-pressed (left) or roll-pressed films (right). The initial undrawn films (A) and (D) were biaxially melt-drawn at 150°C up to *DR* = 4×4 (B) (E) and *DR* = 8×8 (C) (F). Scale bar, 1μm.

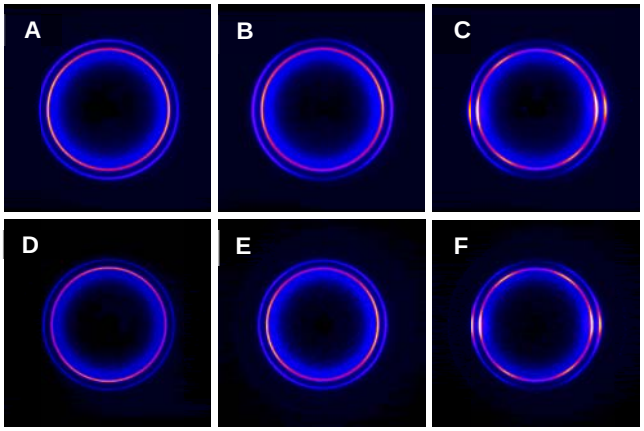

Fig 3 WAXD images edge-viewed for membranes prepared from the powder-pressed (top) and roll-pressed films (bottom). Samples (A) - (F) are same in Fig. 2. Vertical drawing directions in the biaxial membrane preparation were maintained for all images. The inner and outer rings correspond to (110) and (200) reflections for the orthorhombic form.

*DR*s in Fig. 2F. Therefore, the desirable transparency was obtained for the latter series of membranes, as depicted in Fig. 1b. These suggest that the roll-pressing for initial film preparation is effective to erase the powder boundary.

WAXD images were edge-viewed for the membranes biaxially melt-drawn from powder-pressed and roll-pressed films in Fig. 3. Both 4x4 membranes exhibits two arcs oriented on the equator, indicating the oriented ECC formation. In contrast, there are additional 4-point reflections on diagonal directions for both 8x8 membranes. These characteristic diagonal reflections are attributed to the inclined ECCs, due to the membrane shrinkage after biaxial melt-drawing at the higher *DR*. It should be noted that these characteristics are similar at given *DR* for both membranes prepared from powder-pressed and roll-pressed films.

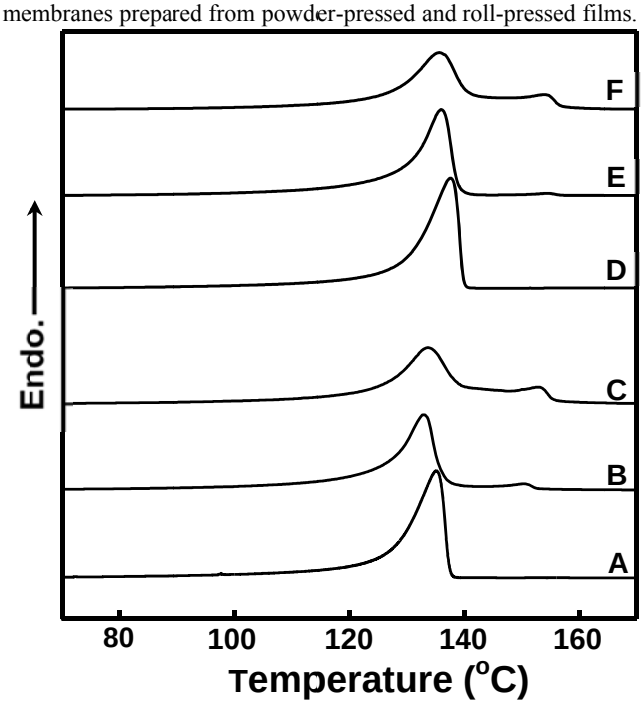

Fig 4 DSC thermograms for UHMW-PE membranes prepared from the powder-pressed (A-C) and roll-pressed films (D-F). Samples (A) - (F) are same in Figs. 2 and 3. The heating rate was 10°C/min.

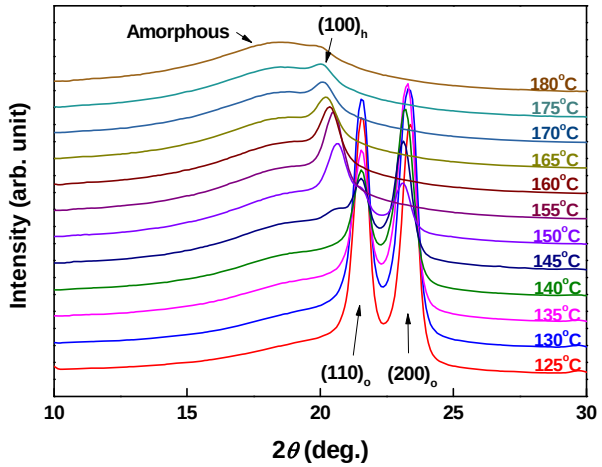

Fig 5 Stacked 2θ line profiles extracted along equatorial direction of a series of *in-situ* WAXD patterns edge-viewed during heating the *DR*=8x8 membrane prepared from the roll-pressed film, which is same as sample (F) in Figs. 2-4. The heating rate was 2°C/min. The measurement temperatures were denoted with the corresponding profiles.

Here, all the through-viewed patterns exhibit random reflection rings for both series of membranes, independent of *DR* (Fig. S1 ESI†). These results suggest that no difference between the membranes prepared from powder-pressed and roll-pressed films was recognizable in WAXD analysis.

Melting behaviour of these membranes are also similar, as depicted in Fig. 4. The characteristic double endotherms are observed for both biaxially melt-drawn membranes prepared from powder-pressed and roll-pressed films. The lower-T_m endotherm is observed for initial films in Figs. 4A and 4D, but the higher-T_m one is characteristic for melt-drawn membranes. The higher biaxial *DR* emphasizes the higher-T_m endotherm, independent of initial film preparation (Figs. 4C and 4F). Similar double melting endotherms have been observed for uniaxially melt-drawn UHMW-PE film,[16-18] These lower- and higher-T_m endotherms are attributable to melting of lamellar FCCs and fibrilar ECCs. However, the peak position of the higher-T_m endotherm is quite different between previous uniaxially and present biaxially melt-drawn samples. The former uniaxially melt-drawn film exhibits the higher-T_m at 144°C,[16-18] but the latter biaxially melt-drawn membrane gives the higher-T_m at 150°C in Figs. 4A and 4F, which exceeds the equilibrium T_m of PE (145°C[33]). Similar higher T_m has been observed for high-strength gel-spun UHMW-PE fibers wounded to copper pieces in a DSC cell.[9] During heating UHMW-PE fibers with fixed ends, fibrillar ECCs are initially orthorhombic form, but transform into mesophase hexagonal one above 150°C.[34] Such hexagonal form is disordered to give the lower melting entropy, which is ascribed to the higher T_m exceeding the equilibrium T_m of closely-packed orthorhombic crystals. *In-situ* X-ray measurements during heating the *DR*=8x8 membrane prepared from roll-pressed film exhibit corresponding phase transition from orthorhombic to hexagonal form, as depicted in Fig. 5. Until 145°C, the orthorhombic (110) and (200) reflections are major, but rapidly disappears at 150°C. Spontaneously, the hexagonal (100) reflection peak newly appears at 150°C. Such hexagonal peak immediately decreases with increasing temperature, due to final melting of the hexagonal ECCs. These results indicate that fibrillar ECCs transform from initial orthorhombic into hexagonal one even for the biaxially melt-drawn UHMW-PE prepared in this study. Such characteristic appearance of hexagonal form in our membrane indicates a fixation effect similar to wounding gel-spun fibre. As shown in Fig. 2C, the radial orientation of fibrillar ECCs parallel to membrane surface is similar to the woven textures, which are constraint each other even during melting. However, the coincident increases of the oriented ECCs in Fig. 2 and the higher-T_m endotherm in Fig. 4 are still independent of initial film preparation.

Such increase of ECCs develops the mechanical properties of these series of biaxially melt-drawn membranes of UHMW-PE. Again, it should be noted that skiving limits the resultant film thickness to 100μm; however, the present study successfully provides much thinner membranes of several micrometres. Fig. 6a depicts the changes in tensile strength and membrane thickness with increasing biaxial *DR* for the membrane prepared

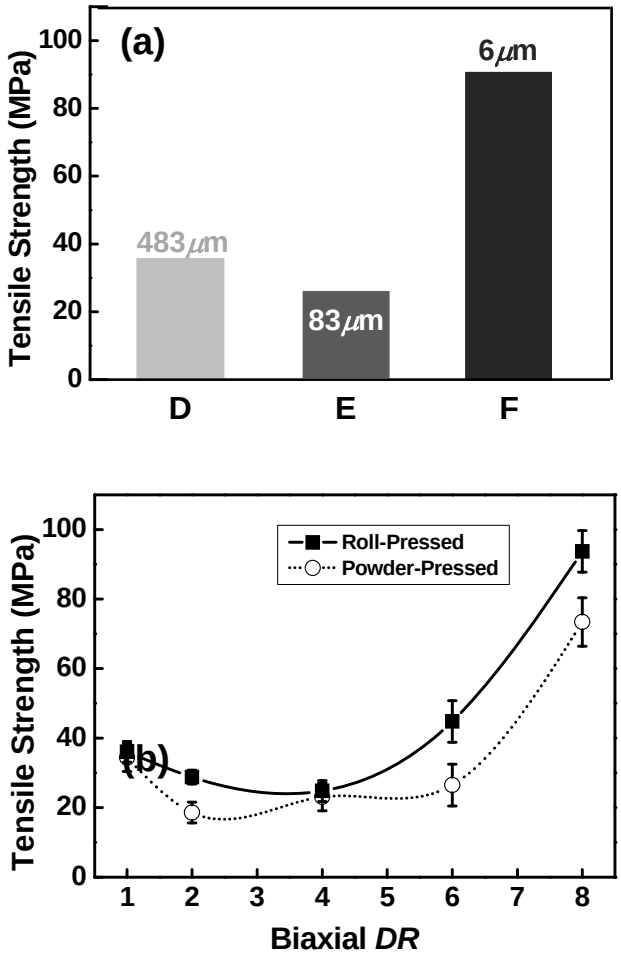

Fig 6 Tensile strength of the UHMW-PE membranes prepared in this study. (a) Corresponding thickness change with stepwise processing. Samples (D) - (F) are same in Figs.2-4. (b) Value change as a function of biaxial *DR*. The results obtained for the targeted roll-pressed films were compared to those for the conventional powder-pressed films. Biaxial melt-drawing was performed at 150°C.

from the roll-pressed film. The initial film had the thickness around 500μm, but it could be thinned below 100μm at biaxial *DR* of 4x4, finally leading to 6μm at 8x8. In contrast, the corresponding tensile strength increases from initial 35MPa to

final 90MPa although the thickness reduction is one of several tens. Here, the thickness measured for several points of the tested membrane was always within a 10% deviation.

As described above, X-ray and DSC results are quite similar for both biaxially melt-drawn membranes prepared from powder-pressed and roll-pressed films. However, the mechanical properties are developed for the latter series of membranes. Fig. 6b compares the tensile strength of the membranes with different biaxial *DR*s drawn from the targeted roll-pressed and conventional powder-pressed films.[28] Tensile strength increases with increasing biaxial *DR* and reaches 90MPa, which is significantly higher than the maximum achievable value of 75MPa for the membrane biaxially melt-drawn from the powder-pressed film. Even at the lower *DR*s, the values for the membranes prepared from roll- pressed films are always higher than those for the powder-pressed film. Here, these strength values for the sample specimens cut along the horizontal, vertical and diagonal directions toward biaxial drawing axes were included in the error bars at the corresponding *DR*s. The above superior physical properties of the former membranes are ascribed to the structural homogeneity of the resultant membrane prepared from the roll-pressed film, which is also confirmed in SEM images in Fig. 2. A combination of roll processing and compression moulding is effective for property development of the resultant biaxially melt-drawn membranes.

Recently, Keller et al.[35,36] reported that protein molecules, which is required for cell proliferation, are effectively absorbed on stacked lamellar surfaces prepared by uniaxial melt-drawing of UHMW-PE. Our biaxial melt-drawing technique is advantageous for preparing UHMW-PE membranes with a larger area (over several hundreds of millimetres square) even at laboratory scale, enabling wider culturing of various cells. The thinness of our membrane also facilitates peeling from the proliferated cell without fracturing damage, which is required for regenerative transportation.

Conclusions

We prepared a series of thin membranes of UHWM-PE by biaxial melt-drawing technique without any solvent treatment. A combination of rolling and compressing successfully erases the powder boundaries within the initial films, resulting in a biaxially melt-drawn membrane with a homogeneous structure. The thickness of the prepared UHMW-PE membrane could be reduced to several micrometres, but its mechanical properties are quite superior to those of the commercial UHMW-PE membranes prepared by the conventional skiving technique.

Acknowledgments

This study was partly supported by the Industrial Technology Research Grant Program from the New Energy and Industrial Technology Development Organization (NEDO) of the Japan and Ogasawara Science and Technology Foundation.

Notes and references

[a]*Division of Molecular Science, Faculty of Science and Technology, Gunma University, Kiryu, Gunma 376-8515, Japan; E-mail: hirokiuehara@gunma-u.ac.jp*

† Electronic Supplementary Information (ESI) available: WAXD images through-viewed for the prepared membranes. See DOI: 10.1039/b000000x/

1 T. A. Tervoort, J. Visjager and P. Smith, *Macromolecules* **2002**, *35*, 8467.
2 T. Aoike, D. Yokoyama, H. Uehara, T. Yamanobe and T. Komoto, *Wear* **2007**, *262*, 742.
3 D. F. Williams, *Biomaterials* **2008**, *29*, 2941.
4 S. M. Kurtz, O. K. Muratoglu, M. Evans and A. A. Edidin, *Biomaterials* **1999**, *20*, 1659.
5 S. Rastogi, L. Kurelec, D. Lippits, J. Cuijpers, M. Wimmer and P. J. Lemstra, *Biomacromolecules* **2005**, *6*, 942.
6 T. Moro, H. Kawaguchi, K. Ishihara, M. Kyomoto, T. Karita, H. Ito, K. Nakamura and Y. Takatori, *Biomaterials* **2009**, *30*, 2995.
7 M. Kyomoto, T. Moro, K. Saiga, M. Hashimoto, H. Ito, H. Kawaguchi, Y. Takatori and K. Ishihara, *Biomaterials* **2012**, *33*, 4451.
8 D.-W. Ihm, J.-G. Noh and J.-Y. Kim, *J. Power. Source* **2002**, *109*, 388.
9 A. J. Pennings and A. Zwijnenburg, *J. Polym. Sci. Polym. Phys. Ed.* **1979**, *17*, 1011.
10 T. Kanamoto, A. Tsuruta, K. Tanaka, M. Takeda and R. S. Porter, *Macromolecules* **1988**, *21*, 470.
11 D. Sawai, K. Nagai, M. Kubota, T. Ohama and T. Kanamoto, *J. Polym. Sci., Polym. Phy. Ed.* **2006**, *44*, 153.
12 P. Pakhomov, S. Khizhnyak, V. Galitsyn, B. Hartmann, E. Moeller, V. Nikitin, V. Zakharov and A. Tshmel, *J. Macromol. Sci., Phys.* **2008**, *47*, 1096.
13 P. Smith, H. D. Chanzy and B. P. Rotzinger, *Polym. Commun.* **1985**, *26*, 258.
14 T. Kanamoto, T. Ohama, K. Tanaka, M. Takeda and R. S. Porter, *Polymer* **1987**, *28*, 1517.
15 S. Rastogi, Y. Yao, S. Ronca,; J. Bos and J. van der Eem, *Macromolecules* **2011**, *44*, 5558.
16 H. Uehara, M. Nakae, T. Kanamoto, A. E. Zachariades and R. S. Porter, *Macromolecules* **1999**, *32*, 2761.
17 M. Nakae, H. Uehara, T. Kanamoto, T. Ohama and R. S. Porter, *J. Polym. Sci., Polym. Phys. Ed.* **1999**, *37*, 1921.
18 M. Nakae, H. Uehara, T. Kanamoto, A. E. Zachariades and R. S. Porter, *Macromolecules* **2000**, *33*, 2632.
19 H. Uehara,; M. Kakiage, T. Yamanobe,; T. Komoto and S. Murakami, *Macromol. Rapid Commun.* **2006**, *27*, 966.
20 M. Kakiage, T. Yamanobe, T. Komoto, S. Murakami and H. Uehara, *J. Polym. Sci., Polym. Phys. Ed.* **2006**, *44*, 2455.
21 M. Kakiage, T. Yamanobe, T. Komoto, S. Murakami and H. Uehara, *Polymer* **2006**, *47*, 8053.
22 M. Kakiage, M. Sekiya, T. Yamanobe, T. Komoto, S. Sasaki, S. Murakami and H. Uehara, *Polymer* **2007**, *48*, 7385.
23 M. Kakiage, M. Sekiya, T. Yamanobe, T. Komoto, S. Sasaki, S. Murakami, and H. Uehara, *J. Phys. Chem. B* **2008**, *112*, 5311.
24 M. Kakiage, H. Uehara and T. Yamanobe, *Macromol. Rapid Commun.* **2008**, *29*, 1571.
25 T. Morioka, M. Kakiage, T. Yamanobe, T. Komoto, H. Kamiya, Y. Higuchi, K. Arai, S. Murakami and H. Uehara, *Macromolecules* **2007**, *40*, 9413.
26 H. Uehara, T. Obana, M. Kakiage, H. Tanaka, H. Masunaga, T. Yamanobe and E. Akiyama, J. Mater. Chem. C, *J. Mater. Chem. C*, DOI:10.1039/C3TC31265H.
27 H. Uehara, Y. Arase, K. Suzuki, Y. Yukawa, Y. Higuchi, Y. Matsuoka and T. Yamanobe, Macromol. Mater. Eng., DOI:10.1002/mame.201300310.
28 H. Uehara, T. Tamura, M. Kakiage and T. Yamanobe, *Adv. Funct. Mater.* **2012**, *22*, 2048.
29 H. Uehara, R. Yoshida, M. Kakiage, T. Yamanobe and T. Komoto, *Ind. Eng. Chem. Res.* **2006**, *45*, 7801.
30 H. Uehara, H. Tanaka, T. Yamanobe, *Polym. J.* **2012**, *44*, 795.
31 J. Suwa, M. Kakiage, T. Yamanobe, T. Komoto and H. Uehara, *Langmuir* **2007**, *23*, 5882.
32 Z. Bashir and A. Keller, *Colloid Polym. Sci.* **1989**, *267*, 116.
33 F. A. Quinn Jr. and L. Mandelkern, *J. Am. Chem. Soc.* **1958**, *80*, 3178.

34 M. Kakiage,; T. Tamura,; S. Murakami,; H. Takahashi and H. Uehara, T. Yamanobe, *J. Mater. Sci.* **2010**, *45*, 2574.
35 T. F. Keller, J. Schönfelder, J. Reichert, Tuccitto, N. Licciardello, A. Messina, G. M. L. Marletta and K. D. Jandt, *ACS Nano* **2011**, *5*, 3120.
36 M. Kastantin, T. F. Keller, K. D. Jandt and D. K. Schwartz, *Adv. Funct. Mater.* **2012**, *22*, 2617.